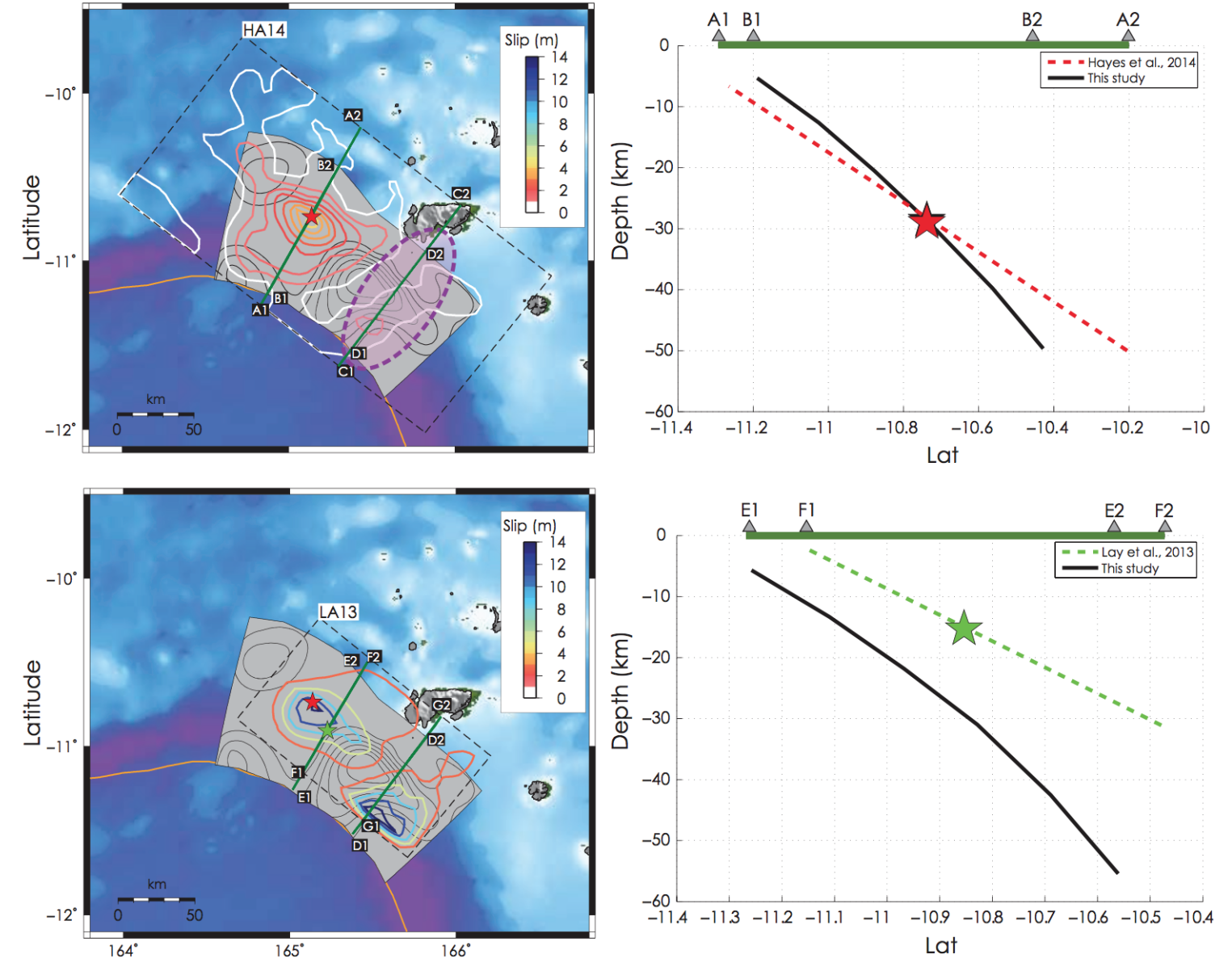


1. Abstract

The scope of this study is to investigate the influence that some details of the seismic source process, namely slip distribution and geometry complexity, have on tsunami generation. In particular, we examine to what extent a tsunami generated by a earthquake is sensitive to rupture complexity or if a simple fault model, i.e. a planar fault, is sufficient for hazard studies.

The study is also motivated by the need to ascertain if accounting for non-planar surfaces is important in the context of slip inversions based on tsunami data. For example, in the case of slip inversion, Lay et al. 2013, Hayes et al. 2014 and Romano et al. 2015 all produced different slip distributions for the same earthquake using different fault geometries (see adjacent figure).

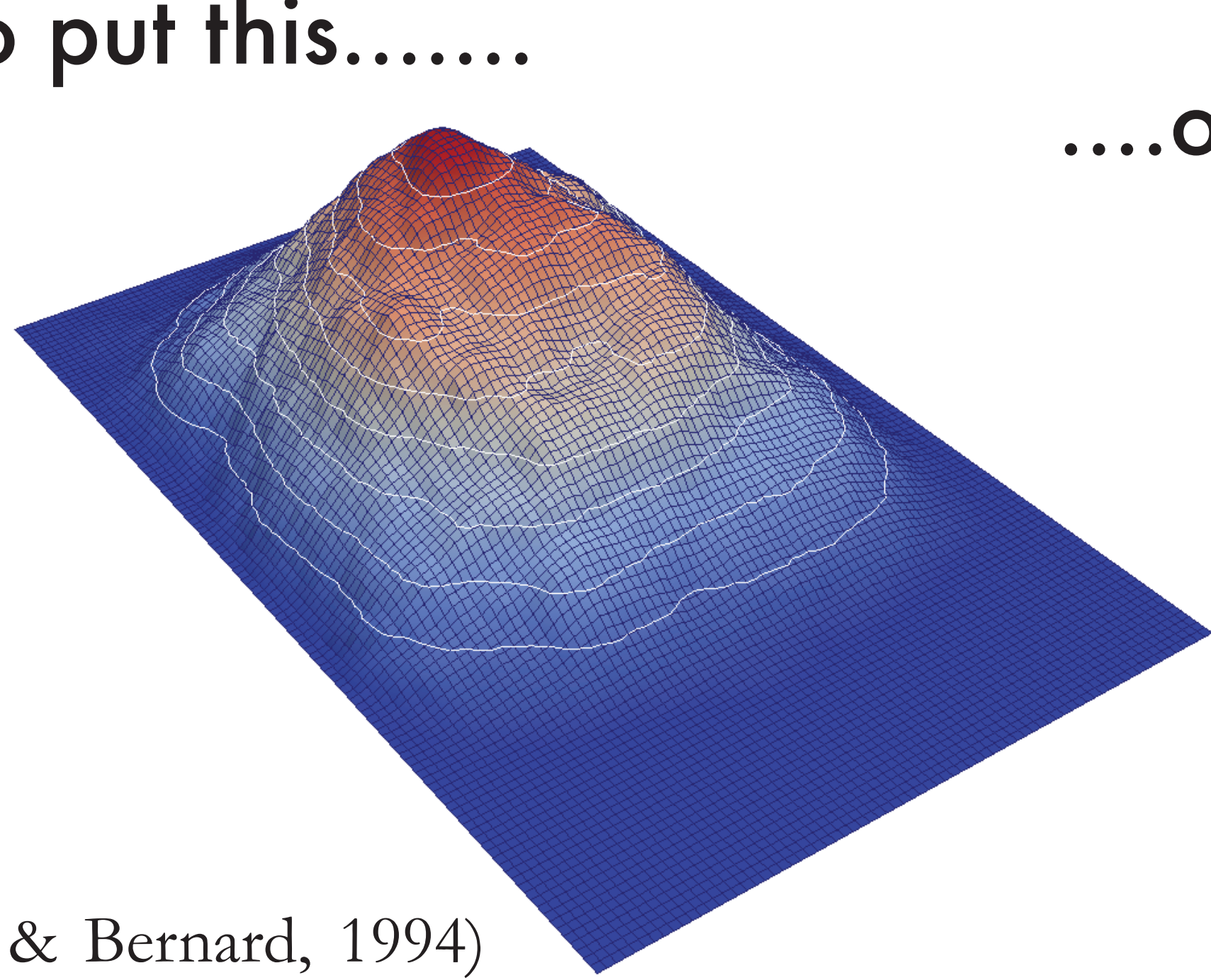


To study this problem, we first need to solve how to distribute a composite source model on a curved fault plane. To do this we compute a geodesic distance matrix, which is an improvement on a classical Dijkstra's algorithm on a complex 2D surface in a 3D space. This distance matrix is then used in a composite source model in order to generate heterogeneous slip distributions with k^2 spectra.

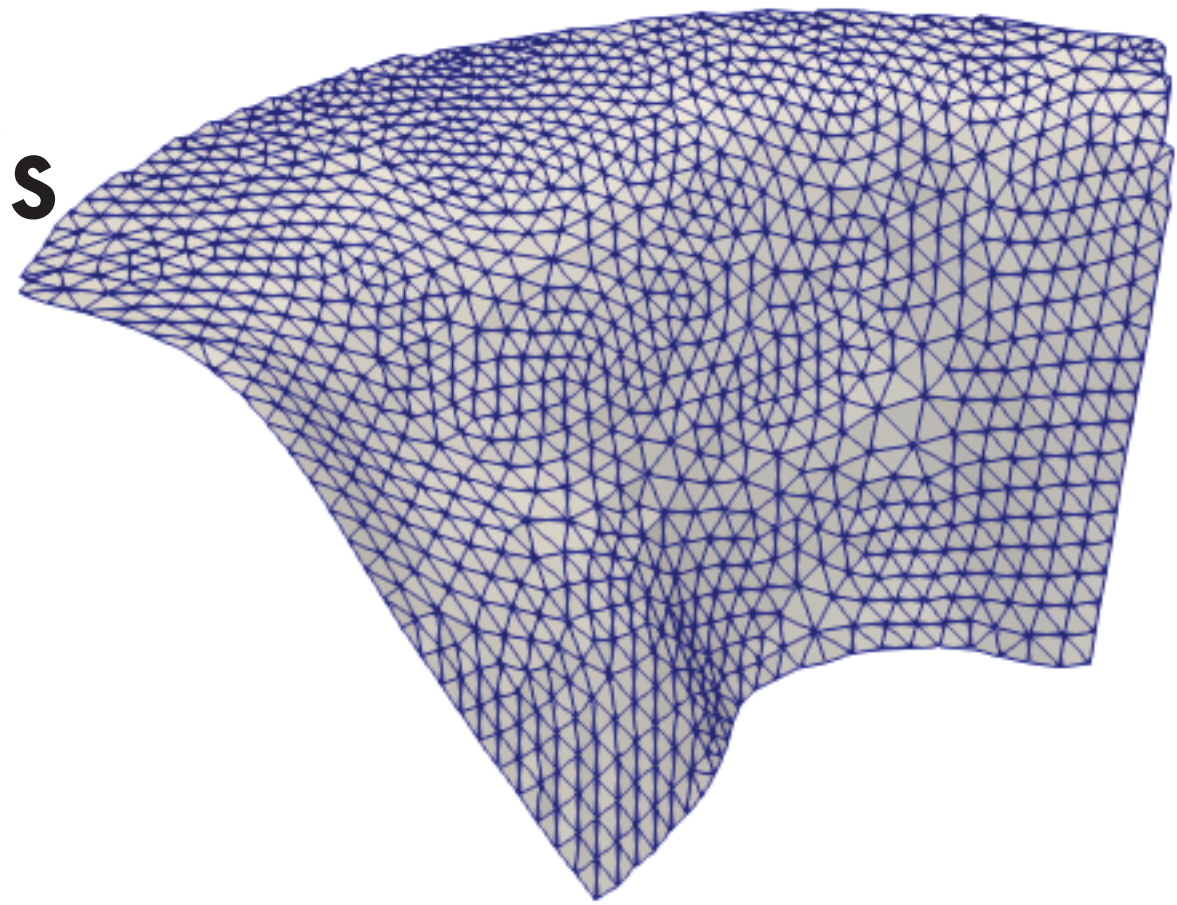
The subduction zones that generated the 2011 M_w 9 Tohoku and 2013 M_w 8 Santa Cruz Islands earthquakes are taken as case studies. Simple rectangular faults and complex 2D fault surfaces based on Slab 1.0 with both uniform slip and k^2 slip are used as source generation for tsunamis. The Tohoku fault will be used to generate three M 9 earthquakes, and the Santa Cruz Island fault will be used to generate three M 8.5 events. Preliminary results will focus on comparing the tsunami wave height observed along nearby coastlines generated by the different source models.

The Problem

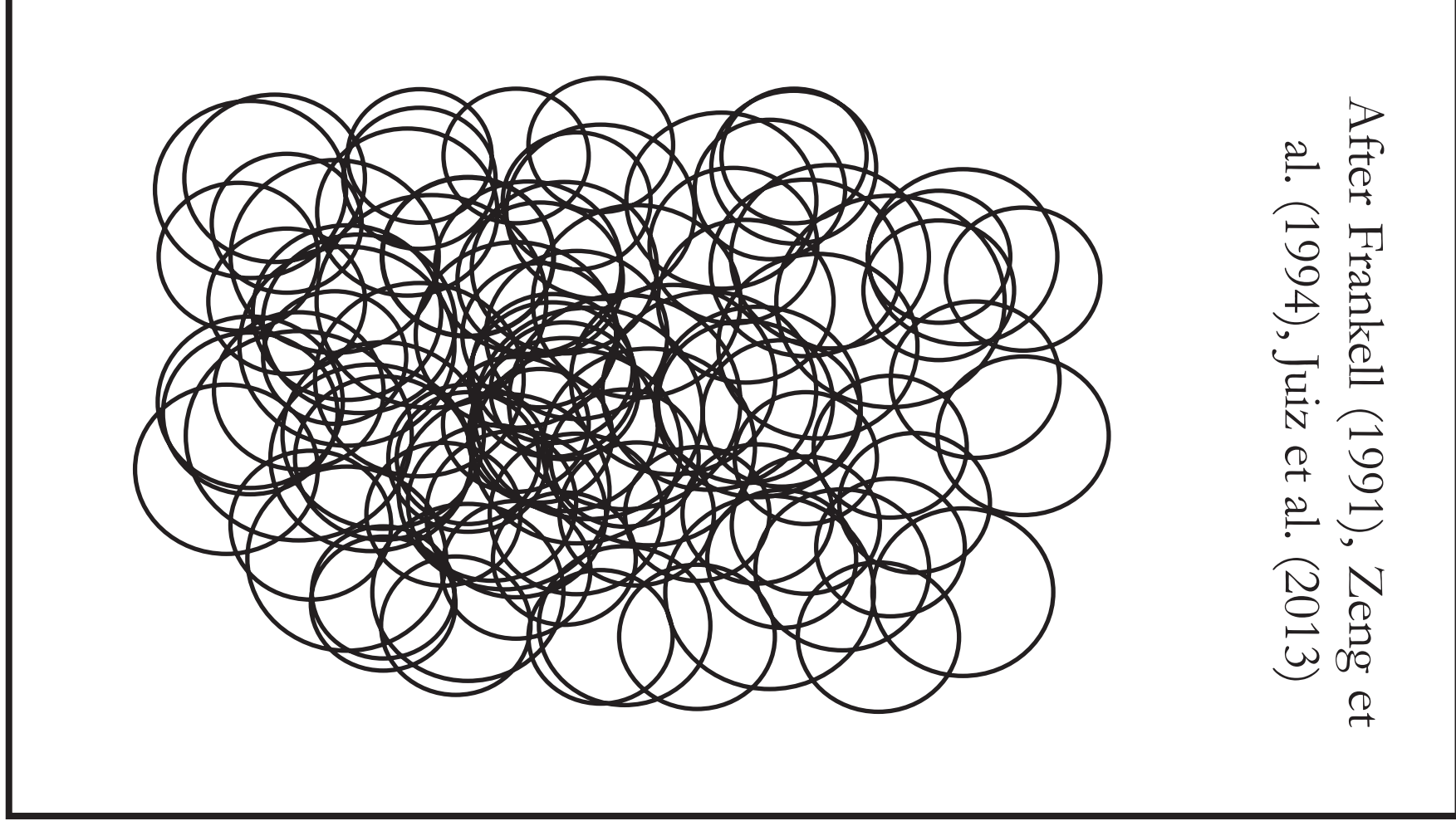
How to put this.....



....on this



Building at k^2 slip distribution



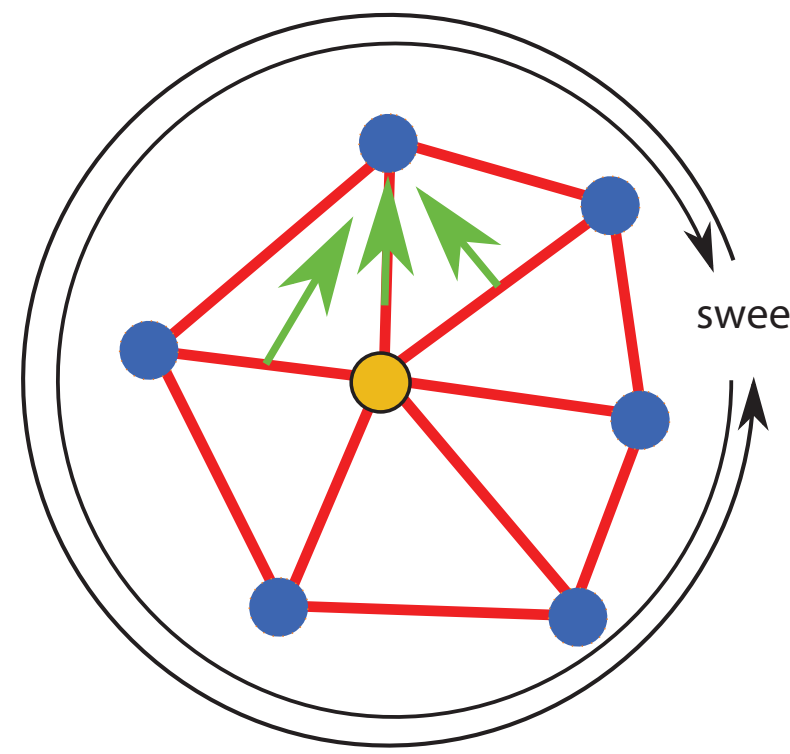
After Frankel (1991), Zeng et al. (1994), Ruiz et al. (2013)

2. Generating k^2 stochastic slip distributions on non-planar faults

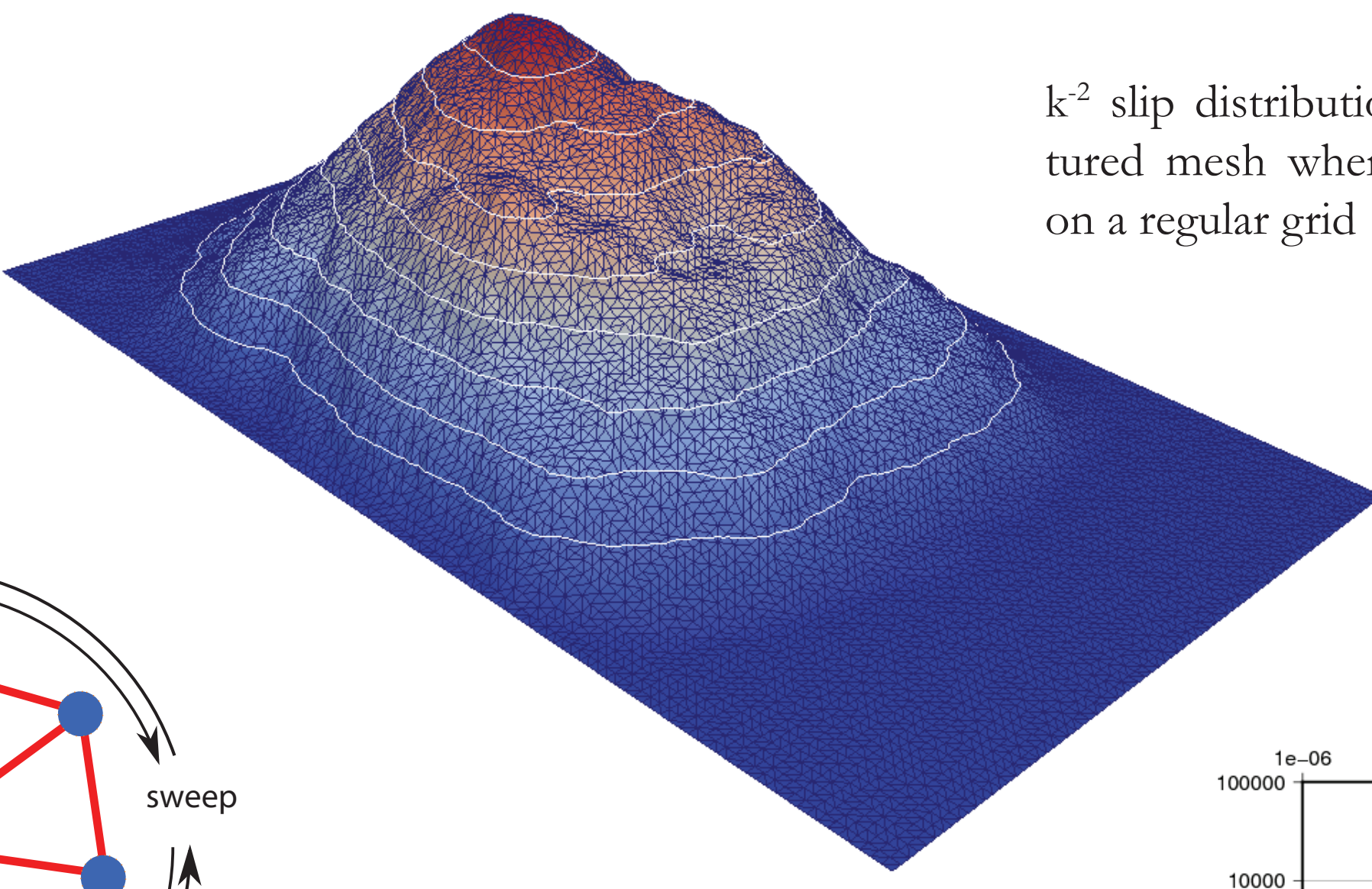
The Solution

Computing the distance with the double lateration solutions after Novotni & Klein (2002)

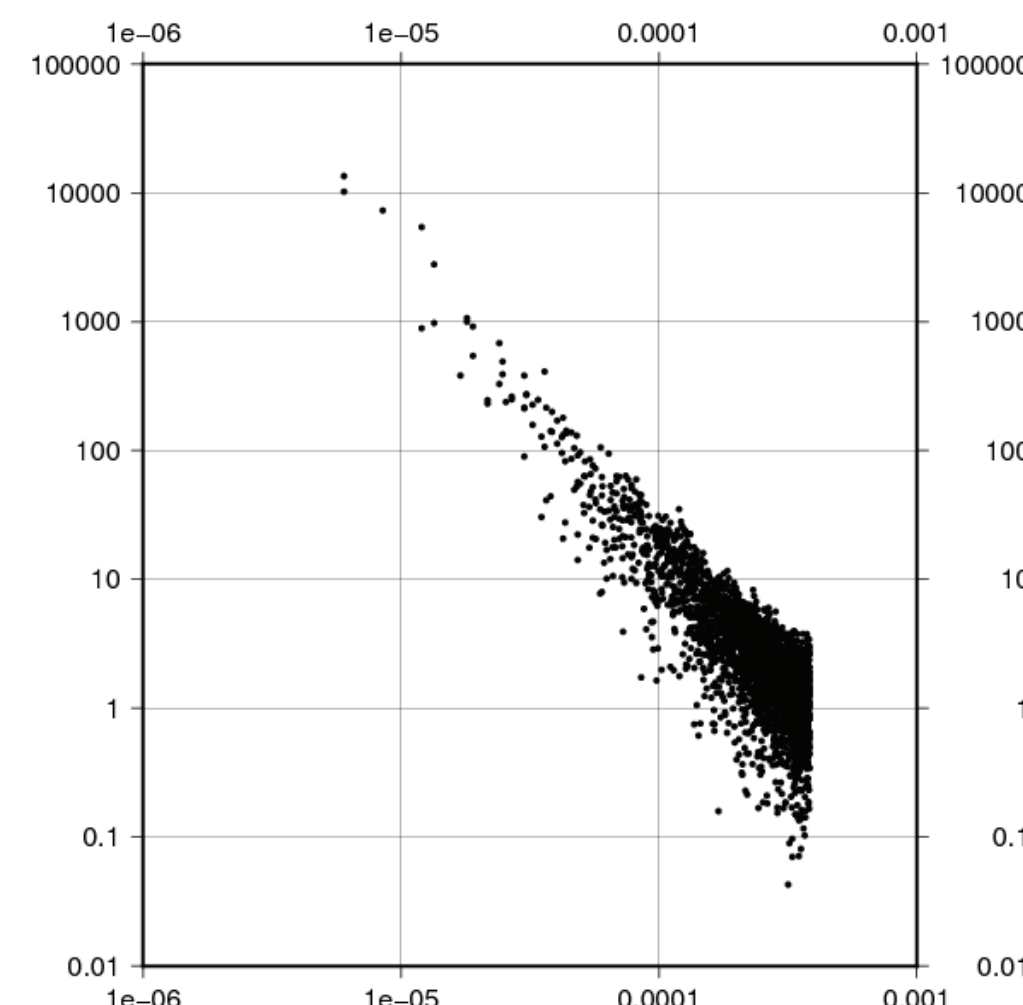
First lateration (green) to locally position the third point of the face
The distance is the length of the red segment



Second lateration (yellow) to position the apparent origin



k^2 slip distribution on an unstructured mesh where the vertices are on a regular grid



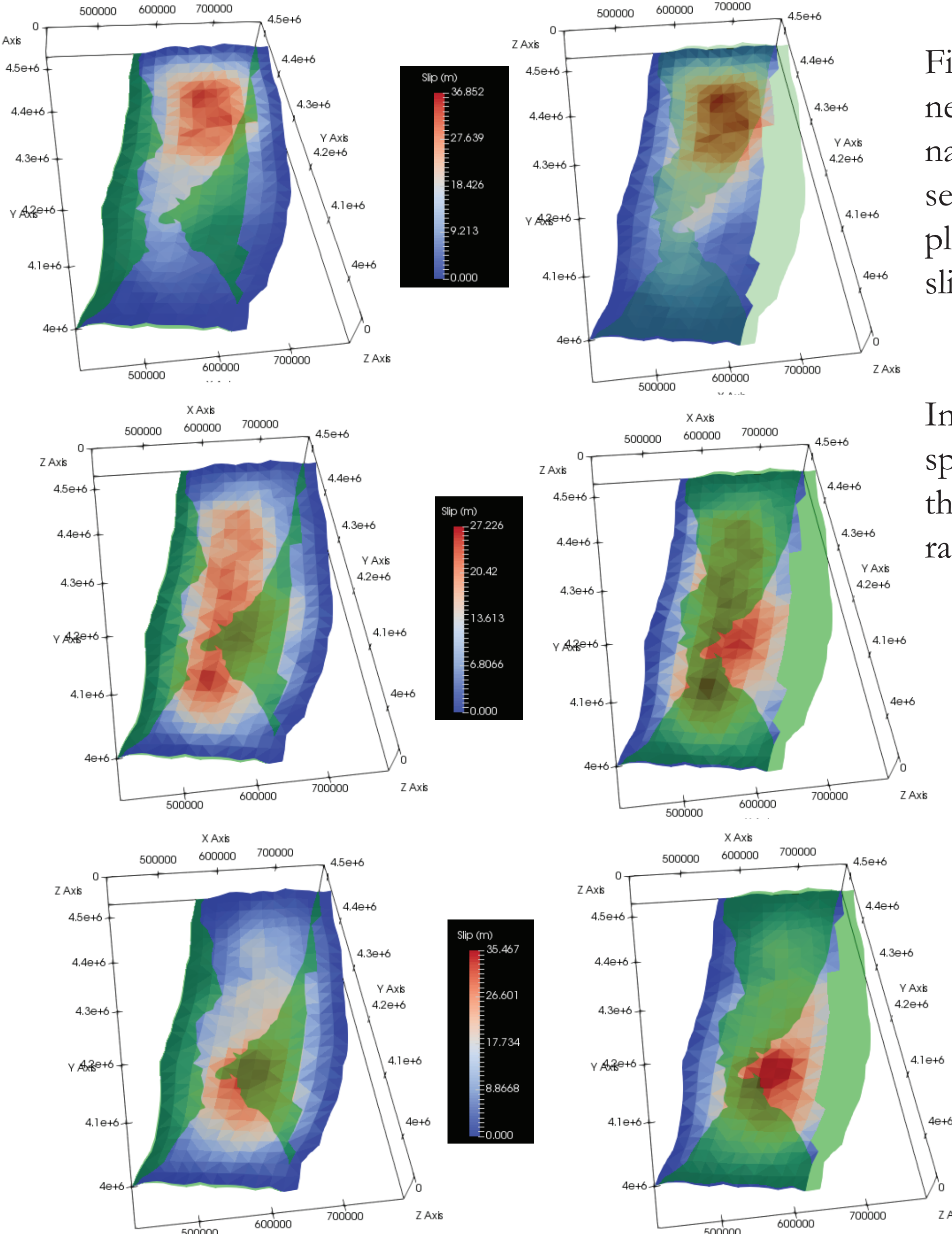
Spectrum of the slip distribution above

3. Comparison between Planar & Non-Planar Faults

3a. Slip Distributions

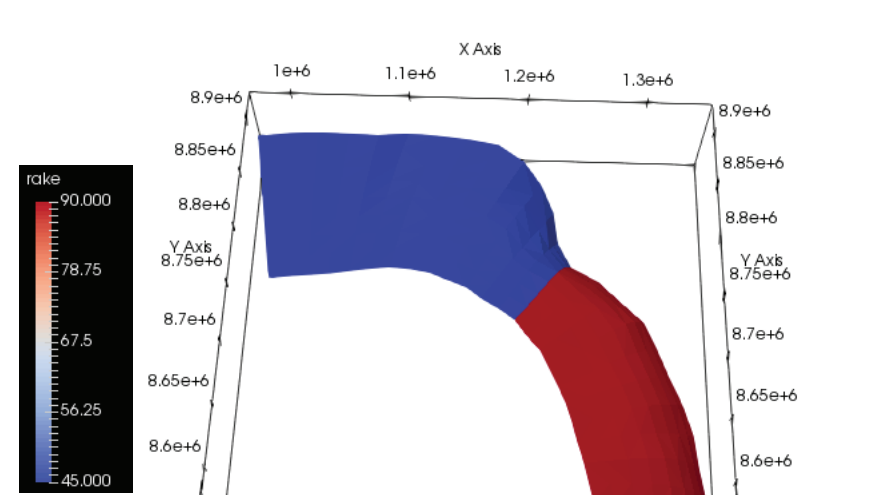
M 9 Tohoku

Non-Planar Fault Planar Fault



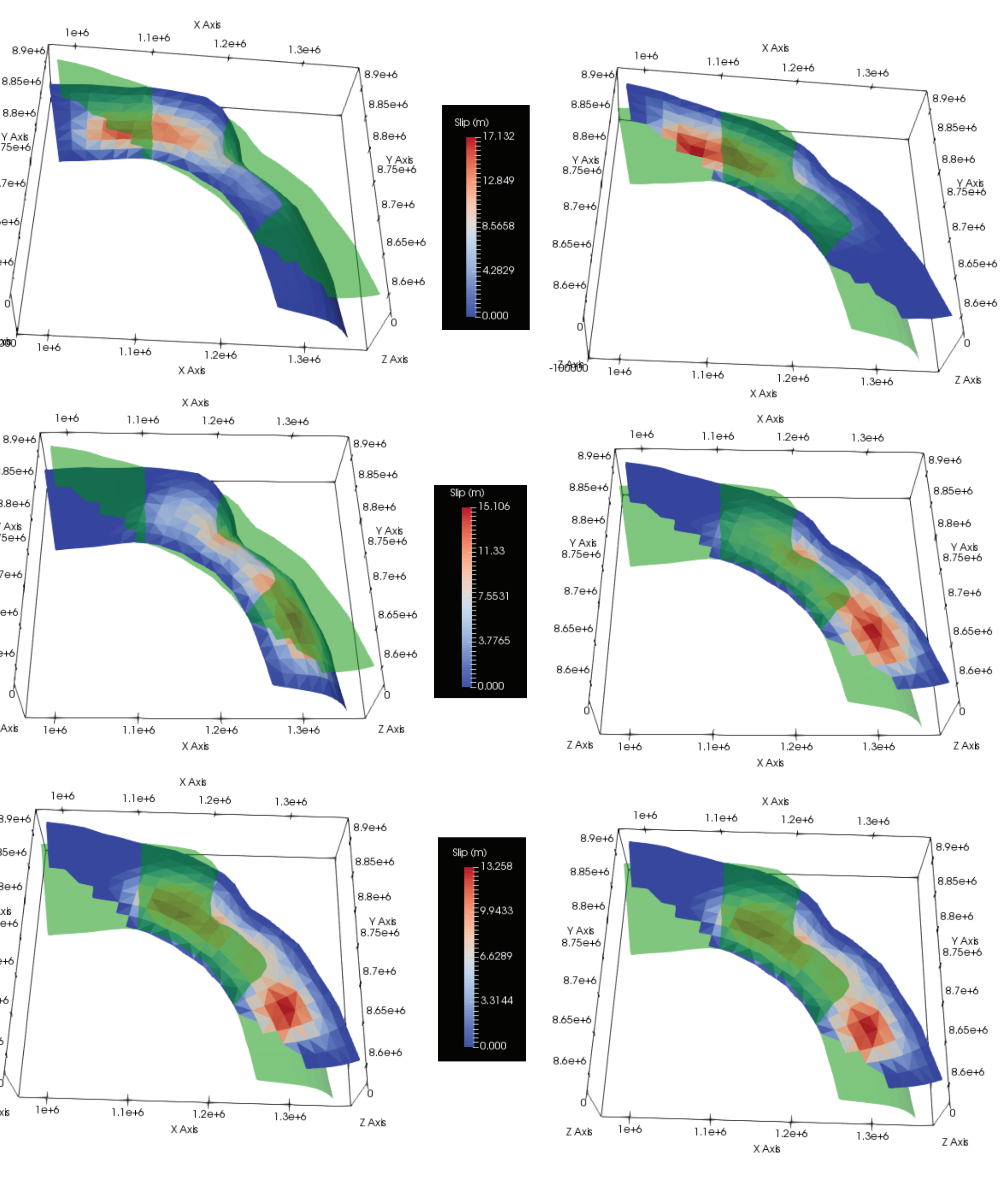
Figures in this section show heterogeneous slip distributions used in the tsunami simulations. Green surface represents the corresponding planar/non-planar fault as reference to the displayed slip distribution.

In the case of Santa Cruz the rake varies spatially across the non-planar fault and this depicted below. In all other cases a rake of 90° is assumed.



M 8.5 Santa Cruz

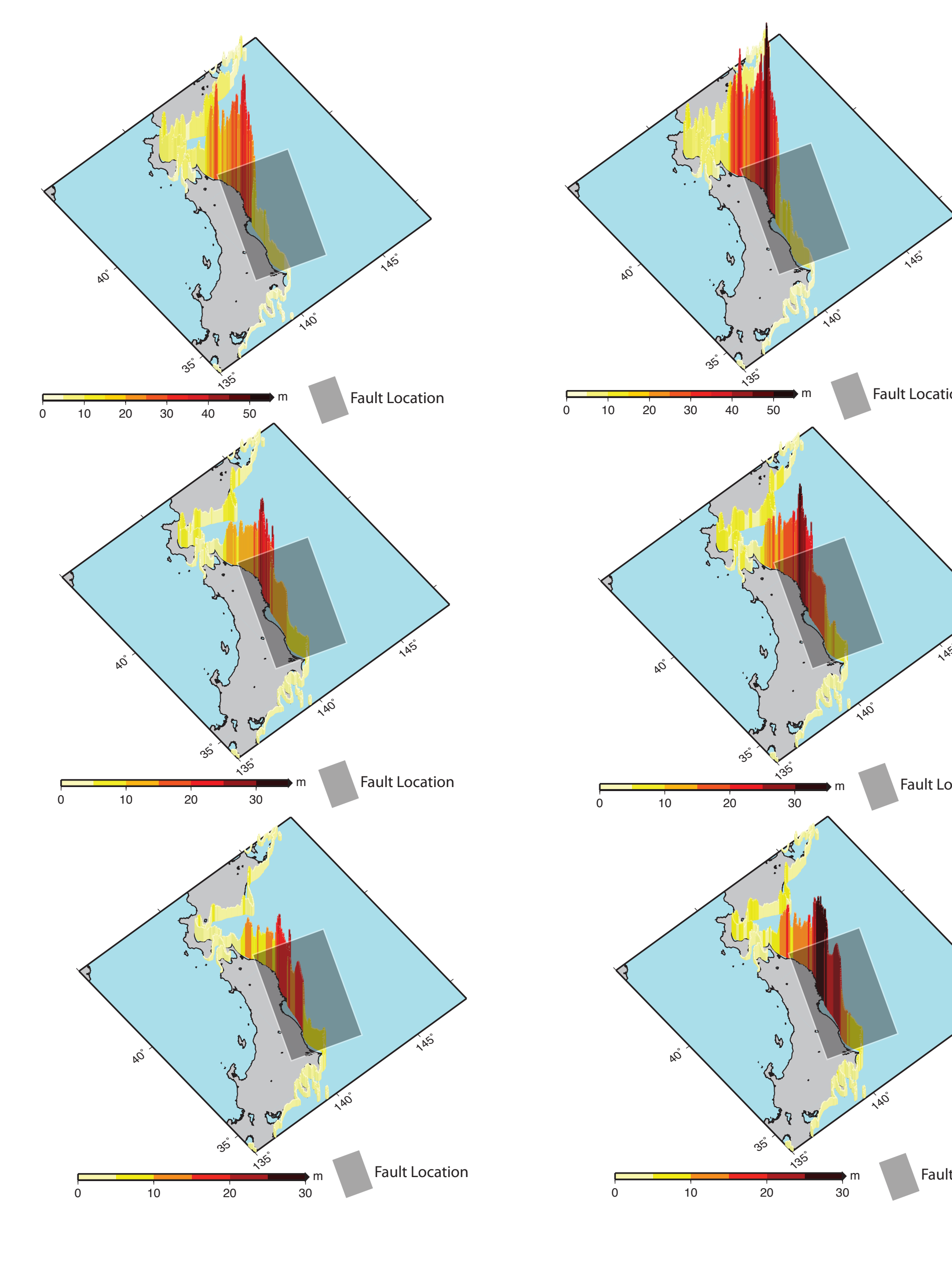
Non-Planar Fault Planar Fault



3b. Tsunami

M 9 Tohoku

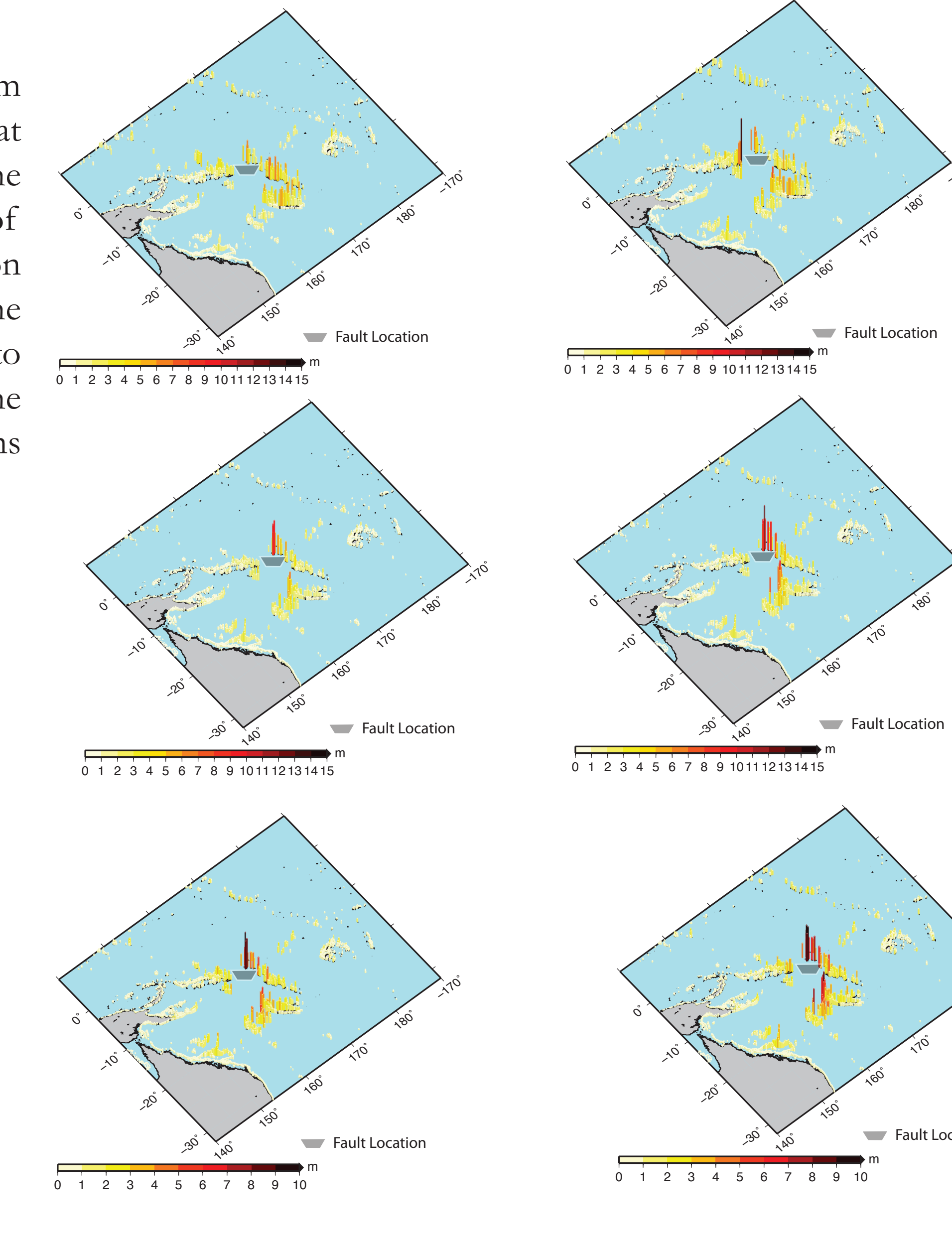
Non-Planar Fault Planar Fault



Figures in this section show maximum tsunami wave amplitude calculated at the 50 m isobath and extrapolated to the shoreline based on an amplification of 2.66 (i.e. the fourth root of 50) based on Green's Law. The figure displaying the slip distribution that corresponds to each of tsunami simulations has the same relative location between sections 3a and 3b.

M 8.5 Santa Cruz

Non-Planar Fault Planar Fault



4. Conclusions

Computing a geodesic distance matrix on a non-planar fault surface and using it with a composite source methodology allows us to produce heterogeneous slip distribution. Using this technique on regularly spaced planar fault produces a slip distribution with a k^2 spectra.

In all case studies, planar faults produce larger offshore tsunami wave amplitudes compared to the same event on a non-planar fault. This is due to a planar fault focusing tsunami wave energy in a particular direction depending on fault strike and dip. In contrast, non-planar faults, with their variable dip and strike tend not to focus the tsunami wave to the same extent.

References

Dijkstra, E. W. (1959). A note on two problems in connexion with graphs. Numer. Math., 1, 269-271.
Frankel, A. (1991). High-Frequency Spectral Falloff of Earthquakes, Fractal Dimension of Complex Rupture, b Value, and the Scaling of Strength on Faults. J. Geophys. Res., 96, 6291-6302.
Herrero, A. & Bernard, P. (1994). A Kinematic Self-Similar Rupture Process for Earthquakes. Bull. Seism. Soc. Am., 84, 1216-1228.
Hayes, G. P., Furlong, K. P., Benz, H. M., and Herman, H. W. (2014). Triggered aseismic slip adjacent to the 6 February 2013 Mw 8.0 Santa Cruz Islands megathrust earthquake, Earth Planet. Sc. Lett., 388, 265-272.
Kimmel, R. & Sethian, J. A. (1998). Computing geodesic paths on manifolds. Proceedings of the National Academy of Sciences, 95, 8431-8435.
Lay, T., Ye, L., Kianmori, H., Yamanaka, Y., Cheung, K. F., & Ammon, C. J. (2013). The February 6, 2013 Mw 8.0 Santa Cruz Islands earthquake and tsunami, Tectonophysics, 608, 1109-1121.
Novotni, M. & Klein, R. (2002). Computing Geodesic Distances on Triangular Meshes: The 10-th International Conference in Central Europe on Computer Graphics, Visualization and Computer Vision'2002 (WSCG2002).
Romano, F., Molinari, I., Lorito, S. & Piatanesi, A. (2015). Source of the 6 February 2013 Mw 8.0 Santa Cruz Islands Tsunami. Nat. Hazards Earth Syst. Sci., 15, 1371-1379.
Zeng, Y., Anderson, J. G. & Yu, G. (1994). A composite source model for computing realistic synthetic strong ground motions. Geophys. Res. Lett., 21, 725-728.